Asian Journal of Chemistry; Vol. 38, No. 2 (2026), 499-516
ASIAN JOURNAL OF CHEMISTRY
https://doi.org/10.14233/ajchem.2026.35210

HR-LCMS based Metabolic Profiling, *in vitro* Analysis and Computational Insight of *Tabernaemontana divaricata* Hydroalcoholic Extract: A Multitargeted Approach to Combat Asthma

UMA MALI[1,*] and RITA CHAKOLE[2]

[1]Department of Pharmaceutics, Tatyasaheb Kore College of Pharmacy, Warananagar-416113, India
[2]Department of Pharmaceutical Chemistry, Government College of Pharmacy, Chhatrapati Sambhaji Nagar-431005, India

*Corresponding author: E-mail: umamali2403@gmail.com

Received: 8 November 2025 *Accepted*: 15 January 2026 *Published online*: 31 January 2026 AJC-22269

Tabernaemontana divaricata (L.) is a prevalent horticultural species in Southeast Asia, also occurring in Australia, tropical Asia and Polynesia shows a diverse range of activities. To explore the molecular mechanisms and targets for prospective and effective therapeutic approaches, molecular docking enables the identification of the most promising targets in asthma. The present study investigates the multitargeted anti-asthmatic potential of phytocompounds isolated from *T. divaricata* by docking analysis. The hydroalcoholic extract of *T. divaricata* (TDHE) was obtained using the Soxhlet extraction and analysed for antiasthmatic activity. Chemical profiling of the extract was carried out using HR LC-MS/MS, which revealed the presence of 19 distinct phytocompounds. All the isolated 19 phytocompounds were docked against prime modulators in asthma such as histamine H1 (PDB: 3RZE), human interleukin-6 (PDB: 1ALU), IL4-IL4R-IL13Ra ternary complex (PDB: 3BPN), IL-25-IL-17RB-IL-17RA ternary complex (PDB: 7UWL), as well as IL-13 (PDB: 5KNH) receptors. The results demonstrated that TDHE possesses significant antiasthmatic potential, primarily through anti-inflammatory and antihistaminic mechanisms. Among the screened phytocompounds, kaempferol-3-O-rutinoside, 8-[4,5-dihydroxy-6-(hydroxymethyl)-3-[3,4,5-trihydroxy-6-(hydroxymethyl)oxan-2-yl]oxyoxan-2-yl]-5,7-dihydroxy-2-(4-hydroxyphenyl)chromen-4-one and selaginpulvilin T exhibited strong binding affinities across all targeted receptors. In addition, ADMET profiling of the identified compounds supported their favourable pharmacokinetic and safety profiles. This study highlights the medicinal potential of *T. divaricata* phytocompounds as alternative or adjunctive therapeutic agents for asthma, offering a multitargeted strategy to modulate immune responses and alleviate disease symptoms. Future investigations should focus on clinical evaluation of the isolated phytocompounds to validate their efficacy and safety in asthma management.

Keywords: *Tabernaemonata divaricata*, Molecular docking, ADMET, Hydroalcoholic extract.

INTRODUCTION

Herbs have been widely used since ancient times to alleviate the symptoms of various inflammation-related disorders. Metabolites derived from these herbs directly interfere with inflammatory processes and response mechanisms, including the production of secondary messengers [1]. *Tabernaemontana divaricata* (L.) is a prevalent horticultural species in Southeast Asia, also occurring in Australia, the Asia tropics and Polynesia [2]. Traditional folk medicine has utilised *T. divaricata* (L.) R. br. for its analgesic, anti-inflammatory, antioxidant, anti-infection and anti-tumor properties [3,4]. *T. divaricata* also exhibits immunomodulatory effects towards *in vivo* and *in vitro* models of asthmatic mice. This endorses an innovative method for the management of allergic and cough-related asthma [5].

Asthma is a chronic inflammatory airway disease characterized by recurrent dyspnoea and wheezing due to bronchoconstriction and allergic inflammation. It affects nearly 300 million individuals worldwide, with an estimated 100 million additional cases expected by 2025 [6]. Standard treatments, including bronchodilators, anti-inflammatory agents and anti-IgE therapies, alleviate airway inflammation and smooth muscle spasm [7]; however, high costs, limited accessibility in low-income regions, and adverse effects such as cardiovascular complications from β_2-agonists and metabolic disturbances from corticosteroids remain major concerns [8,9].

Asthma pathogenesis involves complex genetic, environmental and immunological interactions leading to airway hyperresponsiveness, mucus hypersecretion, inflammatory cell infiltration and airway remodelling [10,11]. Moreover, the computational approaches such as molecular docking (MD) and molecular dynamics simulations play a crucial role in drug discovery by accurately predicting binding affinities between ligands and target proteins. In the context of asthma, molecular docking facilitates the identification of key molecular targets and helps elucidate underlying mechanisms for the development of effective therapeutic strategies [12]. In present research work, we identified the active phytocompounds from the hydroalcoholic extract of *T. divaricata* by HR LC-M/MS analysis and subsequently examined the *in silico* activity of phytocompounds *via* molecular docking and ADMET evaluation against different proteins implicated in asthma for a multitargeted treatment.

EXPERIMENTAL

Upper portions of *Tabernaemontana divaricata* were collected from the Western Ghats of Maharashtra state of India. The plant was verified by the Botanical Survey of India, Pune. The leaves of the plants were detached, cleaned with distilled water, shade-dried and then pulverised into coarse powder.

Extraction: The hydroalcoholic extract of *T. divaricata* leaves (TDHE) was prepared using a Soxhlet extractor. Leaves powder (600 g) was initially defatted with petroleum ether in the Soxhlet apparatus at 65 °C to remove waxy components, followed by extraction with 1200 mL of a 50:50 ethanol-water mixture. The resulting hydroalcoholic extract was dried at 40 ± 2 °C to obtain a solid mass, which was subsequently stored in a suitable glass container. The extraction yielded 43.8 g of dried extract, corresponding to a 7.3% yield [13].

In vitro activity

Anti-inflammatory activity using protein denaturation: A 10 mL reaction mixture was prepared containing 0.4 mL of fresh hen egg albumin, 5.6 mL of phosphate-buffered saline (PBS, pH 6.4) and 100 µL of the test solution at various concentrations. Double-distilled water was used as control. The mixtures were initially incubated at 37 ± 2 °C for 15 min, followed by heating at 70 °C for 5 min. After cooling, the absorbance of each sample was measured at 660 nm, using solvent as a blank. Diclofenac sodium at varying concentrations was used as the reference standard and subjected to the same procedure for absorbance measurement [14,15]. The % protein denaturation inhibition was determined using the following equation:

$$\text{Inhibition } (\%) = \frac{Q - P}{Q}$$

where P= absorbance of the sample of test, Q = absorbance of sample of control.

Anti-inflammatory potential using HRBC membrane stabilisation method: Blood samples were collected from a volunteer who had avoided the NSAIDs for approximately 14 days prior to the study. The samples were centrifuged at 7000 rpm for 5 min and the supernatant was discarded. The concentrated blood cells were washed with isotonic saline and a 10% suspension was prepared. TDHE, at concentrations ranging from 20 to 100 µg/mL in buffer, was each mixed with 2 mL of 0.36% hyposaline and 0.5 mL of HRBC suspension. The mixtures were incubated at room temperature for 10 min, followed by centrifugation at 2800 rpm for 5 min. The absorbance of the supernatant was measured at 540 nm. Aspirin, at concentrations of 20, 40, 60, 80 and 100 µg/mL, was used as the standard. The percentage of HRBC membrane stabilization was calculated using the following formula [16].

$$\text{Hemolysis } (\%) = \frac{OD_T}{OD_C} \times 100$$

$$\text{Protection } (\%) = 1 - \frac{OD_T}{OD_C} \times 100$$

where OD_T = optical concentration of the test sample and OD_C represents the optical density of the negative control.

Anti-histaminic activity by goat tracheal chain method: The trachea of a goat was obtained from an abattoir and dissected into individual rings, which were then connected sequentially to form a chain. The tracheal rings were suspended in a 30 mL organ bath containing Tyrode's solution and maintained at 37 ± 0.5 ºC with continuous aeration. Each ring was equilibrated under a 400 mg load for approximately 45 min, with fresh Tyrode's solution added at 15 min intervals. The contraction responses were induced using histamine (500 µg/mL) to establish baseline tension. The percentage relaxation of histamine-induced contraction was measured in the presence of the standard drug salbutamol and the test extract (TDHE) at concentrations ranging from 0.1 to 2 mg/mL. Data were analyzed using a t-test to assess the statistical significance of relaxation effects [17].

Phytochemicals estimation by HR LC-MS/MS: The identification of polar bioactive compounds was conducted *via* the Agilent 6200 with TOF/6500 series Q-TOF B.09.00 (B9044.0) liquid chromatography paired with a mass spectrometer, including electron ionisation, also a fused silica DB-5 column (30 m × 0.25 mm) with 0.25 µm thickness of film. Heat of the oven was sustained at 50 ºC for 5 min and subsequently programmed to rise from 50 ºC to 280 ºC for about 40 min. The mobile phase comprising a chloroform-methanol-water solvent system at a ratio of 1:5:4 mL was administered, possessing a flow rate (2 mL/min). A distribution ratio (1:30) was employed for the injection of a 1 µL sample and the ionisation voltage for analysis of Mass spectra was conducted using the EI technique concerning 70 eV. The compounds were identified by correlating their mass spectrometry with standards retention index data and ethnic spectra and by comparing their fragmentation patterns in mass spectra with those in LIB, WILEY 139 and NIST 12.LIB (3), which are spectral libraries utilised for the identification of chemical compounds [18].

Molecular docking: Molecular docking was performed *via* AutoDock Vina incorporated into PyRx 0.8, with ligands and target proteins selected through the Vina Wizard module. A maximised grid box was employed to enable blind docking over the entire surface of the protein, ensuring an unbiased search for potential sites of binding. The exhaustiveness para-

meter was set to eight to enhance conformational sampling and docking accuracy. The top-ranked binding poses were selected depending on binding affinity and further analysed for molecular interactions. Visualisation and interpretation of ligand-protein interactions were performed using BIOVIA Discovery Studio to elucidate key binding residues and interaction profiles.

The 3D crystal structures of histamine H1 receptor (PDB: 3RZE), human interleukin-6 (PDB: 1ALU), IL4-IL4R-IL13Ra ternary complex (PDB: 3BPN), IL-25-IL-17RB-IL-17RA ternary complex (PDB: 7UWL), as well as sIL-13 (PDB: 5KNH) were selected as molecular targets based on prior studies [19-23]. The selected protein structures were fetched from the Protein Data Bank (RCSB) and preprocessed in BIOVIA Discovery Studio by detaching heteroatoms, molecules of water and non-essential co-factors. Polar hydrogens were added to optimize the residue in tautomeric states [24]. The protein structures were transformed into an AutoDock compatible macromolecule format following energy minimisation.

***In silico* drug-likeness and ADMET assessment:** The drug-likeness and ADMET profile were assessed utilizing the SwissADME and pkCSM online servers [25,26].

RESULTS AND DISCUSSION

The hydroalcoholic extract of *T. divaricata* leaves was analysed by HR LC-MS/MS utilizing a Q-TOF high-resolution mass spectrometer to thoroughly assess its phytochemical composition. Table-1 provides a comprehensive summary of the isolated compounds, detailing their retention times, experimental *m/z* values, calculated masses, molecular formulae and pubmed ID of the molecules, thereby revealing the presence of diverse secondary metabolites such as terpenoids, phenols, flavonoids, alkaloids and related phytochemical classes [27].

Anti-inflammatory potential *via* protein denaturation method: The anti-inflammatory activity of TDHE (20-100 µg/mL) was evaluated by assessing its ability to inhibit albumin denaturation, using diclofenac sodium as reference standard. TDHE exhibited a concentration-dependent inhibitory effect on albumin denaturation, as shown in Fig. 1, with inhibition values ranging from 12.63 ± 0.36% to 51.42 ± 0.17% across the tested concentration range. Significantly, TDHE demonstrated appreciable anti-inflammatory activity at the lower concentration of 20 µg/mL, comparable to diclofenac sodium and showed a significant increase in inhibitory activity relative to the standard at higher concentrations.

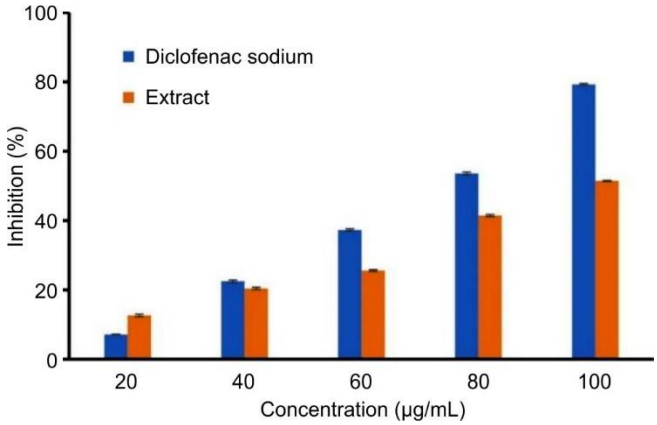

Fig. 1. % Inhibition of protein denaturation by THDE

Anti-inflammatory potential through HRBC membrane stabilisation method: The reduction of hypotonicity-derived lysis of red blood cell membranes of humans, which is similar to lysosomal membrane components, was utilised as an indicator of the anti-inflammatory efficacy of medi-

TABLE-1
LIST OF PHYTOCHEMICALS OBTAINED FROM LCMS CHEMICAL PROFILING OF TDHE

Name	RT left (min)	m.f.	Ontology	m.w.	PubChem ID
Sorbate	0.042	$C_6H_8O_2$	Medium-chain fatty acids	2067.19	1549237
Shikimate	0.042	$C_7H_{10}O_5$	Shikimic acids and derivatives	34.62	8742
Quinic acid	0.042	$C_7H_{12}O_6$	Quinic acids and derivatives	2381.48	6508
D-(+)-Trehalose	0.042	$C_{12}H_{22}O_{11}$	O-Glycosyl compounds	181.33	7427
Selaginpulvilin T	0.042	$C_{36}H_{28}O_5$	Fluorenes	84.5	137178
5-Hydroxytryptophan	0.497	$C_{11}H_{12}N_2O_3$	Serotonins	414.09	144
Spectinomycin	1.205	$C_{14}H_{24}N_2O_7$	1,4-Dioxanes	23.69	15541
Altenusin	2.419	$C_{15}H_{14}O_6$	Biphenyls and derivatives	1893.5	6918469
Harman	2.571	$C_{12}H_{10}N_2$	Harmala alkaloids	34.75	5281404
Kaempferol-3-O-rutinoside	3.784	$C_{27}H_{30}O_{15}$	Flavonoid-3-O-glycosides	16570.79	5318767
2',4'-Dihydroxy-4-methoxychalcone	3.177	$C_{16}H_{14}O_4$	2'-Hydroxychalcones	8940.59	5711223
8-[4,5-Dihydroxy-6-(hydroxymethyl)-3-[3,4,5-trihydroxy-6-(hydroxymethyl)oxan-2-yl]oxyoxan-2-yl]-5,7-dihydroxy-2-(4-hydroxyphenyl)chromen-4-one	6.007	$C_{27}H_{30}O_{15}$	Flavonoid 8-C-glycosides	6078.7	74977780
Methyl-13-hydroperoxy-delta9E,11E-octadecadienoate	7.17	$C_{19}H_{34}O_4$	Lineolic acids and derivatives	1097.95	6439850
Phosphatidylcholine lyso alkyl 18	7.372	$C_{26}H_{56}NO_6P$	Monoalkylglycerophosphocholines	7987.67	134736196
Hydroquinidine	7.018	$C_{20}H_{26}N_2O_2$	Cinchona alkaloids	1700.15	91503
7,4'-Dimethoxyisoflavone	10.253	$C_{17}H_{14}O_4$	7-O-methylisoflavones	6257.7	466269
9-Hydroxy-10,12-octadecadienoic acid	10.05	$C_{18}H_{32}O_3$	Lineolic acids and derivatives	22.49	5282945
Cholestane	9.899	$C_{27}H_{48}$	Cholestane steroids	115.63	6857534
Lignoceric acid	11.213	$C_{24}H_{48}O_2$	Very long-chain fatty acids	1937.94	11197

cines. TDHE, at a range from 20 µg/mL up to 100 µg/mL, safeguards membranes of human erythrocytes from lysis caused by hypotonic solutions. Fig. 2 depicts the HRBC membrane stabilisation produced by varying concentrations of TDHE. At a concentration of 100 µg/mL, TDHE inhibited 60.97% of RBC haemolysis, whereas aspirin at the same dose exhibited inhibition of 93.45 ± 0.01%. The results obtained demonstrated that the sample TDHE can positively and concentrations dependently inhibit haemolysis of HRBC.

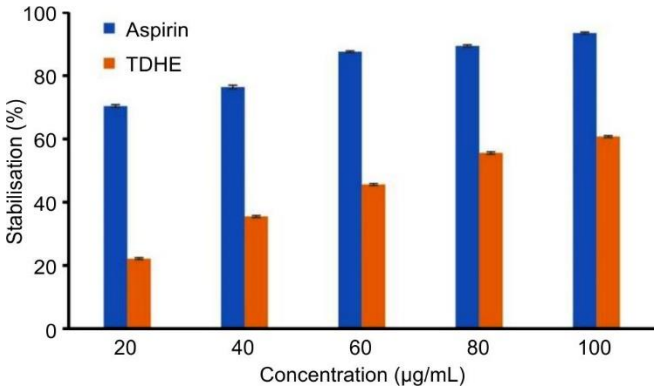

Fig. 2. Percent HRBC membrane stabilisation by THDE

Anti-histaminic activity by goat tracheal chain method: Histamine, at a dosage of 500 µg/mL, induced contraction of the goat trachea. TDHE at lower concentrations did not induce any activity of relaxation activity when studied independently on chains of the trachea of goats. The TDHE at a dosage of 2 mg/mL exhibited a maximum relaxation of 84.44 ± 0.03 ($p < 0.05$) of pre-contracted goat trachea with histamine. At the same concentration, standard salbutamol showed a relaxation of 95.55%. The influence of TDHE at varying amounts of 0.01-2.00 mg/mL on the contraction of trachea of goat induced by histamine is shown in Fig. 3. The test extract produced a dose-dependent relaxation of histamine-constricted goat tracheal tissue, with TDHE exhibiting maximal relaxant activity at a concentration of 2 mg/mL.

Docking studies: The docking analysis at molecular level of the selected ligands in opposition to histamine H1 receptor (PDB: 3RZE), human interleukin-6 (PDB: 1ALU), IL4-IL4R-IL13Ra ternary complex (PDB: 3BPN), IL-25-IL-17RB-IL-17RA ternary complex (PDB: 7UWL) as well as IL-13 (PDB: 5KNH) demonstrated strong binding affinities, indicating favourable interactions with the target proteins. All compounds exhibited stable docking poses within the binding pockets, forming key interactions such as hydrogen bonding, interactions of hydrophobic interactions, along with the π-π stacking with essential residues of the active site. Binding energy values and interaction profiles suggest a high potential for these ligands to modulate the activity of the respective targets.

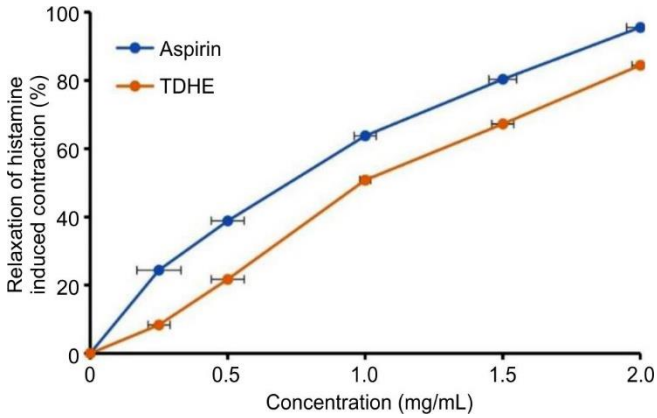

Fig. 3. Percent relaxation of histamine-induced contraction on the goat tracheal chain by THDE and salbutamol

H1 receptor (PDB: 3RZE): The results revealed diverse binding interactions amongst the tested ligands as well as the target protein (PDB: 3RZE; Table-2, Fig. 4), with binding affinities varying from -4.9 to -7.9 kcal/mol. Between the studied compounds, kaempferol-3-O-rutinoside demonstrated the greatest binding affinity (-7.9 kcal/mol), followed by 9-hydroxy-10,12-octadecadienoic acid (-7.7 kcal/mol), selaginpulvilin T (-7.6 kcal/mol), along with cholestane (-7.5 kcal/mol). These high-affinity ligands engaged in multiple hydrogen bonding, π-π stacking, as well as hydrophobic interactions, contributing to their strong binding to the target. Kaempferol-3-O-rutinoside interacted *via* conventional hydrogen bonds with Asn472, Arg125 and Ser128, as well as alkyl and π-alkyl interactions with Arg139 and Lys412, suggesting a stable binding within the active site. Similarly, 9-hydroxy-10,12-octadecadienoic acid formed hydrogen bonds with Lys179 while

TABLE-2
INTERACTION OF PHYTOCOMPOUNDS WITH THE H1 RECEPTOR (PDB: 3RZE)

Code	BA	Interacting residues	Type of interactions	Distance
Lignoceric acid	-4.9	Pro161	Conventional hydrogen bond	2.67
		Trp158	Alkyl, π-Alkyl	4.10
		Leu157	Alkyl, π-Alkyl	5.39, 5.40
		Leu154	Alkyl, π-Alkyl	4.79, 5.16, 5.19
		Pro202	Alkyl, π-Alkyl	3.98
		Phe119	Alkyl, π-Alkyl	4.65, 4.92
		Pro161	Alkyl, π-Alkyl	4.75, 5.09
		Phe190	Alkyl, π-Alkyl	5.32
		Ile197	Alkyl, π-Alkyl	4.29, 5.35
		Phe116	Alkyl, π-Alkyl	5.09
		Leu201	Alkyl, π-Alkyl	4.80, 5.29
		Leu205	Alkyl, π-Alkyl	4.68

Phosphatidylcholine lyso alkyl 18	-5.1	Thr1026	Conventional hydrogen bond	2.03
		Gly1030	Conventional hydrogen bond	2.97
		Glu1011	Conventional hydrogen bond	2.84
		Asp1010	Conventional hydrogen bond	3.38
		Phe1104	π-Sigma	3.59
		Ala1074	Alkyl	4.21
		Leu1032	Alkyl	4.08
5-Hydroxytryptophan	-5.8	Asp183	Conventional hydrogen bond	2.77
		Gly164	Conventional hydrogen bond	2.25
		Trp165	Conventional hydrogen bond	2.47
		Phe190	π-Sigma	3.61
		His167	π-π T-Shaped	4.76
		Val187	π-Alkyl	4.46, 4.55
Quinic acid	-5.5	Arg176	Conventional hydrogen bond	2.46, 2.49
		Glu447	Conventional hydrogen bond	2.16, 2.94
		Asn443	Conventional hydrogen bond	2.45, 2.96
		Asp178	Conventional hydrogen bond	3.51
D-(+)-Trehalose	-6.3	Arg1137	Conventional hydrogen bond	2.02
		Ser1117	Conventional hydrogen bond	2.24, 2.35
		Thr1115	Conventional hydrogen bond	2.49
		Gly1113	Conventional hydrogen bond	2.95
		Gly1110	Conventional hydrogen bond	2.46
		Leu1133	Conventional hydrogen bond	2.80
		Ser1136	Conventional hydrogen bond	2.72
		Gly1113	Conventional hydrogen bond	2.90
Shikimate	-5.2	Asp1070	Conventional hydrogen bond	2.24, 2.51
		Phe1104	Conventional hydrogen bond	2.14
		Phe1104	Conventional hydrogen bond	2.69
Spectinomycin	-6.5	Ala1073	Conventional hydrogen bond	2.45
		His1031	π-Sigma	3.70
Hydroquinidine	-6.3	Val217	Conventional hydrogen bond	3.49
		Ala414	Amide-π Stacked	4.52
		Lys412	Alkyl, π-Alkyl	5.21
		Lys415	Alkyl, π-Alkyl	3.88, 4.27, 4.42
		Ala414	Alkyl, π-Alkyl	4.13
		His220	Alkyl, π-Alkyl	4.94
		Arg411	Alkyl, π-Alkyl	3.85, 5.09
7,4'-Dimethoxyisoflavone	-7.3	Arg97	π-Cation	4.44, 4.51
		Tyr185	π-π T-Shaped	5.27
		Arg175	Alkyl, π-Alkyl	5.21
		Tyr185	Alkyl, π-Alkyl	4.89
		Leu101	Alkyl, π-Alkyl	5.23
		Cys180	Alkyl, π-Alkyl	4.79
		Cys100	Alkyl, π-Alkyl	4.89
		Trp93	Alkyl, π-Alkyl	4.64
		Arg97	Alkyl, π-Alkyl	3.96
Sorbate	-5.3	Ser111	Conventional hydrogen bond	2.97
		Trp158	Alkyl, π-Alkyl	4.98
		Tyr108	Alkyl, π-Alkyl	5.24
		Phe435	Alkyl, π-Alkyl	4.51
		Ala195	Alkyl, π-Alkyl	4.17
		Phe432	Alkyl, π-Alkyl	5.02, 5.30
Harman	-6.7	Gly164	Conventional hydrogen bond	2.55
		Val187	π-Alkyl	4.87, 4.96, 5.02

9-Hydroxy-10,12-octadecadienoic acid	-7.7	Lys179	Conventional hydrogen bond	1.77
		Phe432	Alkyl, π-Alkyl	4.79, 5.31
		Trp428	Alkyl, π-Alkyl	4.81, 5.10
		Phe199	Alkyl, π-Alkyl	5.03
		Ile115	Alkyl, π-Alkyl	4.32
		Phe424	Alkyl, π-Alkyl	5.36
		Tyr431	Alkyl, π-Alkyl	5.03
		Tyr108	Alkyl, π-Alkyl	5.00
		Ile454	Alkyl, π-Alkyl	3.72
		Lys179	Alkyl, π-Alkyl	3.82
Kaempferol-3-*o*-rutinoside	-7.9	Asn472	Conventional hydrogen bond	2.57, 2.74
		Arg125	Conventional hydrogen bond	2.56
		Ser128	Conventional hydrogen bond	2.50
		Glu410	Conventional hydrogen bond	3.60
		Arg139	Alkyl, π-Alkyl	4.00
		Lys412	Alkyl, π-Alkyl	5.42
2',4'-Dihydroxy-4-methoxychalcone	-6.7	Ser1117	Conventional hydrogen bond	2.16
		Asn1116	Conventional hydrogen bond	2.91
		Gly1113	Conventional hydrogen bond	2.46
		Phe1114	π-π T-Shaped	4.60
		Phe1114	π-π Stacked	4.76
		Met1106	Alkyl	4.16
Methyl-13-hydroperoxy-delta9E,11E-octadecadienoate	-5.7	Trp158	π-Sigma	3.71
		Trp158	Alkyl, π-Alkyl	4.64
		Pro161	Alkyl, π-Alkyl	4.51, 4.72, 4.78
		Phe190	Alkyl, π-Alkyl	3.99, 4.60, 5.19
		Phe184	Alkyl, π-Alkyl	4.73
Cholestane	-7.5	Phe156	π-Sigma	3.89
		Trp152	π-Sigma	3.87
		Leu157	Alkyl	4.96
		Leu149	Alkyl	5.30
		Val71	Alkyl	4.76
Altenusin	-6.2	Asn474	Conventional hydrogen bond	2.11, 2.26
		Asn472	Conventional hydrogen bond	2.52
		Ala413	Alkyl, π-Alkyl	4.17, 4.33
		Arg409	Alkyl, π-Alkyl	5.31
8-[4,5-Dihydroxy-6-(hydroxymethyl)-3-[3,4,5-trihydroxy-6-(hydroxymethyl)oxan-2-yl]oxyoxan-2-yl]-5,7-dihydroxy-2-(4-hydroxyphenyl)chromen-4-one	-7.4	Arg56	Conventional hydrogen bond	2.81
		Lys57	Conventional hydrogen bond	2.71
		Asn63	Conventional hydrogen bond	3.03
		Asn472	Conventional hydrogen bond	1.80
		Lys57	Conventional hydrogen bond	2.37
		Arg409	Conventional hydrogen bond	2.72, 2.80
		Thr60	Conventional hydrogen bond	3.56
		Thr60	π-Sigma	2.54
		Lys57	Amide-π Stacked	4.98
Selaginpulvilin T	-7.6	Tyr210	Conventional hydrogen bond	2.37
		Lys415	Conventional hydrogen bond	2.43
		Tyr214	π-π Stacked	3.77
		Gly418	π-π T-Shaped	4.84
		Phe419	Amide-π Stacked	5.01
		Met421	Amide-π Stacked	5.24
		Ile425	Alkyl, π-Alkyl	4.38
		Leu207	Alkyl, π-Alkyl	5.08
		Met421	Alkyl, π-Alkyl	4.70
		Ala422	Alkyl, π-Alkyl	3.71, 3.99
		Lys415	Alkyl, π-Alkyl	5.31

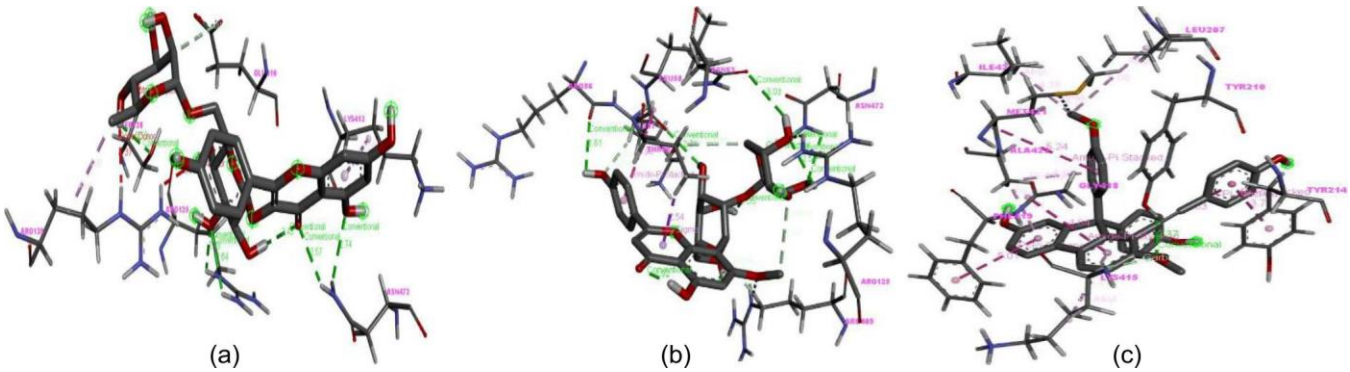

Fig. 4. 3D interaction images of (a) kaempferol-3-*o*-rutinoside, (b) 8-[4,5-dihydroxy-6-(hydroxymethyl)-3-[3,4,5-trihydroxy-6-(hydroxymethyl)oxan-2-yl]oxyoxan-2-yl]-5,7-dihydroxy-2-(4-hydroxyphenyl)chromen-4-one and (c) selaginpulvilin T with H1 receptor (PDB: 3RZE)

exhibiting hydrophobic interactions with multiple residues such as Phe432, Trp428 and Ile115, which may play a crucial role in its strong binding. Selaginpulvilin T (-7.6 kcal/mol) displayed a combination of hydrogen bonding (Tyr210), C-H bonding (Lys415) and π-π stacking (Tyr214, Gly418), along with amide-π stacked interactions with Phe419 and Met421. These interactions highlight the role of aromatic residues in stabilizing the ligand binding. Cholestane (-7.5 kcal/mol) also demonstrated strong π-sigma and alkyl interactions with Phe156, Trp152 and Leu157, indicating its potential for hydrophobic stabilisation. Other notable ligands such as 7,4′-dimethoxyisoflavone (-7.3 kcal/mol) and 8-[4,5-dihydroxy-6-(hydroxymethyl)chromen-4-one (-7.4 kcal/mol) exhibited favourable binding interactions through π-cation, π-π stacking, in addition with hydrogen bonding, emphasizing their potential as lead molecules. Furthermore, spectinomycin (-6.5 kcal/mol), harman (-6.7 kcal/mol), as well as hydroquinidine (-6.3 kcal/mol) displayed moderate binding, primarily facilitated by hydrogen bonding and hydrophobic interactions.

Human interleukin-6 (PDB: 1ALU): The docking results for ligands interacting with PDB: 1ALU revealed significant variations in binding affinities and interaction types (Table-3). Among the studied compounds, kaempferol-3-O-rutinoside showed the greatest binding affinity (-7.9 kcal/mol), creating multiple hydrogen bonds with SER107, LYS46 and ARG104. Moreover, it demonstrated CH bonding with GLU106 including ARG104, along with π-cation and π-anion interactions, suggesting a strong and stable binding to the target protein. Cholestane (-6.9 kcal/mol) also displayed a high binding affinity, primarily through π-sigma and alkyl interactions with residues such as PHE74, LYS66 and MET67, indicating strong hydrophobic interactions contributing to stability. Other

TABLE-3
INTERACTION OF PHYTOCOMPOUNDS WITH HUMAN INTERLEUKIN-6 (PDB: 1ALU)

Code	BA	Interacting residues	Type of interactions	Distance
Lignoceric acid	-3.9	ASP140	Conventional hydrogen bond	2.12
		PRO139	Conventional hydrogen bond	3.03
		THR143	Conventional hydrogen bond	2.36
		TYR97	Alkyl, Pi-Alkyl	5.43
		LEU147	Alkyl, Pi-Alkyl	4.37, 4.43, 4.67
		LYS150	Alkyl, Pi-Alkyl	4.34
Phosphatidylcholine lyso alkyl 18	-4.8	ARG104	Conventional hydrogen bond	2.71, 1.89
		SER107	Conventional hydrogen bond	2.13
		ASP160	Conventional hydrogen bond	2.23
		ARG104	Conventional hydrogen bond	3.57
		LYS46	Alkyl	5.43
5-Hydroxytryptophan	-6.2	THR43	Conventional hydrogen bond	2.16
		ARG104	Conventional hydrogen bond	2.21, 2.30
		ASP160	Conventional hydrogen bond	2.00, 2.00
		ARG104	Pi-Cation	4.59, 4.56
		ASP160	Pi-Anion	3.35
		LYS46	Pi-Sigma	2.78
		LYS46	Pi-Alkyl	5.49
Quinic acid	-5.8	THR43	Conventional hydrogen bond	1.80
		ARG104	Conventional hydrogen bond	1.74, 2.73
D-(+)-trehalose	-5.8	THR43	Conventional hydrogen bond	2.10
		ARG104	Conventional hydrogen bond	2.90
		SER107	Conventional hydrogen bond	2.40
		ASP160	Conventional hydrogen bond	2.77

Shikimate	-5.3	GLU42	Conventional hydrogen bond	2.93
		SER107	Conventional hydrogen bond	2.92
		GLU106	Conventional hydrogen bond	2.15
		ARG104	Conventional hydrogen bond	2.01
		ASP160	Conventional hydrogen bond	1.94
		THR43	Conventional hydrogen bond	2.71
Spectinomycin	-6.1	ARG104	Conventional hydrogen bond	3.09
		GLU106	Conventional hydrogen bond	1.83
		PHE105	Conventional hydrogen bond	2.69
		ARG104	Alkyl, Pi-Alkyl	4.41
		PHE105	Alkyl, Pi-Alkyl	4.18
Hydroquinidine	-6.3	THR43	Conventional hydrogen bond	3.02
		LYS46	Conventional hydrogen bond	3.56
		ASP160	Pi-Cation	3.22, 3.97
		ARG104	Pi-Anion	4.35, 4.45
		LYS46	Alkyl, Pi-Alkyl	4.04
7,4'-Dimethoxyisoflavone	-5.9	PRO139	Conventional hydrogen bond	2.44
		LEU147	Alkyl, Pi-Alkyl	3.76, 4.65
		PRO139	Alkyl, Pi-Alkyl	5.11
		LYS150	Alkyl, Pi-Alkyl	4.03
Sorbate	-4.2	LYS46	Salt Bridge	2.98
		GLU106	Conventional hydrogen bond	2.21
		SER107	Conventional hydrogen bond	1.84
		ARG104	Alkyl, Pi-Alkyl	4.83, 4.50
		PHE105	Alkyl, Pi-Alkyl	4.29, 4.26
Harman	-6.1	ARG182	Pi-Sigma	2.58
		ILE25	Alkyl, Pi-Alkyl	3.90, 5.44
		LYS129	Alkyl, Pi-Alkyl	5.22
		LEU181	Alkyl, Pi-Alkyl	3.78, 4.55
		ARG182	Alkyl, Pi-Alkyl	5.01
9-Hydroxy-10,12-octadecadienoic acid	-4.4	LYS86	Conventional hydrogen bond	2.50
		PRO65	Conventional hydrogen bond	3.00
		LYS66	Alkyl	4.12, 4.16, 4.44
		ALA68	Alkyl	4.64
		LEU64	Alkyl	5.01, 5.20
		LEU165	Alkyl	4.40
Kaempferol-3-*o*-rutinoside	-7.9	SER107	Conventional hydrogen bond	2.46
		LYS46	Conventional hydrogen bond	2.21
		ARG104	Conventional hydrogen bond	2.68, 2.80, 2.93
		GLU106	Conventional hydrogen bond	3.77
		ARG104	Conventional hydrogen bond	2.39
		LYS46	Pi-Cation	4.97
		ASP160	Pi-Anion	4.06, 4.62
		LYS46	Pi-Alkyl	4.84, 4.95
2',4'-Dihydroxy-4-methoxychalcone	-5.9	ASN63	Conventional hydrogen bond	2.48
		TYR97	Pi-Pi T-Shaped	5.38
		LEU147	Alkyl, Pi-Alkyl	4.07
		LYS150	Alkyl, Pi-Alkyl	3.88
Methyl-13-hydroperoxy-delta9E,11E-octadecadienoate	-4.3	ARG104	Conventional hydrogen bond	2.66
		GLN156	Conventional hydrogen bond	2.32
		ASP160	Conventional hydrogen bond	2.26
		LYS46	Alkyl, Pi-Alkyl	4.45, 5.38
		PHE105	Alkyl, Pi-Alkyl	4.42
Cholestane	-6.9	PHE74	Pi-Sigma	3.61
		LYS66	Alkyl, Pi-Alkyl	4.13
		MET67	Alkyl, Pi-Alkyl	5.13
		PHE74	Alkyl, Pi-Alkyl	5.20

Altenusin	-6.6	THR43	Conventional hydrogen bond	2.46
		GLN156	Conventional hydrogen bond	2.80
		ASP160	Conventional hydrogen bond	2.06
		ARG104	Pi-Cation	4.83
		LYS46	Pi-Alkyl	3.86
8-[4,5-Dihydroxy-6-(hydroxymethyl)-3-[3,4,5-trihydroxy-6-(hydroxymethyl)oxan-2-yl]oxyoxan-2-yl]-5,7-dihydroxy-2-(4-hydroxyphenyl)chromen-4-one	-7.2	LYS66	Conventional hydrogen bond	2.77
		GLU172	Conventional hydrogen bond	2.29
		SER176	Conventional hydrogen bond	2.52, 2.75
		ARG179	Conventional hydrogen bond	2.72, 2.07
		PHE74	Pi-Pi Stacked	4.27, 4.09, 5.43
Selaginpulvilin T	-6.2	LYS27	Conventional hydrogen bond	3.01
		LEU178	Conventional hydrogen bond	3.64
		ILE29	Conventional hydrogen bond	2.62
		LEU33	Alkyl, Pi-Alkyl	4.70
		ARG182	Alkyl, Pi-Alkyl	5.41
		LEU178	Alkyl, Pi-Alkyl	4.03, 4.87, 4.93

ligands showing favourable binding included 8-[4,5-dihydroxy-6-(hydroxymethyl)-3-[3,4,5-trihydroxy-6-(hydroxymethyl)-oxan-2-yl]oxyoxan-2-yl]-5,7-dihydroxy-2-(4-hydroxyphenyl)-chromen-4-one (-7.2 kcal/mol), which exhibited multiple hydrogen bonds with LYS66, GLU172, SER176 and ARG179, along with π-π stacking with PHE74. Altenusin (-6.6 kcal/mol) formed conventional hydrogen bonds with THR43, GLN156 and ASP160, while interacting *via* π-cation and π-alkyl bonds, reinforcing its moderate binding stability. Selaginpulvilin T (-6.2 kcal/mol) formed hydrogen bonds with LYS27 and exhibited CH bonding and alkyl interactions with LEU178, ILE29 and ARG182, indicating a balance between hydrophilic and hydrophobic interactions. Similarly, 5-hydroxytryptophan (-6.2 kcal/mol) engaged in multiple hydrogen bonds with THR43, ARG104 and ASP160, along with π-cation and π-anion interactions, contributing to its moderate binding affinity. Spectinomycin (-6.1 kcal/mol) formed hydrogen bonds with ARG104 and GLU106 while establishing alkyl interactions with PHE105. Hydroquinidine (-6.3 kcal/mol) interacted primarily through CH bonds with THR43 and LYS46 and π-cation and π-anion interactions with ASP160 and ARG104, signifying a mixture of electrostatic and hydrophobic stabilisation. Other notable ligands, such as 7,4′-dimethoxyisoflavone (-5.9 kcal/mol) and shikimate (-5.3 kcal/mol), exhibited moderate binding through a mixture of hydrogen bonds, CH bonds, as well as alkyl interactions. Conversely, compounds such as lignoceric acid (-3.9 kcal/mol) and sorbate (-4.2 kcal/mol) demonstrated relatively weaker binding affinities, predominantly forming CH bonds and alkyl interactions, suggesting less stable interactions with the protein (Fig. 5).

IL4 (PDB: 3BPN): Molecular docking of selected compounds with PDB: 3BPN revealed diverse interaction profiles, suggesting varying binding affinities as well as interaction strengths with the target protein (Table-4). Among the studied ligands, 8-[4,5-dihydroxy-6-(hydroxymethyl)-3-[3,4,5-trihydroxy-6-(hydroxymethyl)oxan-2-yl]oxyoxan-2-yl]-5,7-dihydroxy-2-(4-hydroxyphenyl)chromen-4-one exhibited the upmost binding affinity (-9.2 kcal/mol), attached with multiple conventional hydrogen bonds with Pro124, Lys12, Tyr127, Leu319, Asp324 and Lys318, along with additional π-cation, π-sigma and π-alkyl interactions, indicating strong stabilisation within the binding site. Similarly, cholestane (-8.6 kcal/mol) along with kaempferol-3-O-rutinoside (-8.1 kcal/mol) also demonstrated significant binding potential through extensive alkyl and hydrogen bonding interactions, particularly with Lys84, Lys77 and Leu39 in cholestane and Gln106, Glu103 and Thr30 in kaempferol-3-O-rutinoside. Compounds such as 7,4′-dimethoxyisoflavone (-7.2 kcal/mol) and altenusin (-7.1 kcal/mol) formed stable interactions primarily through conventional hydrogen bonding and π-alkyl interactions, suggesting moderate binding stability. Hydroquinidine (-6.4 kcal/mol) and harman (-6.6 kcal/mol) also engaged key residues, notably

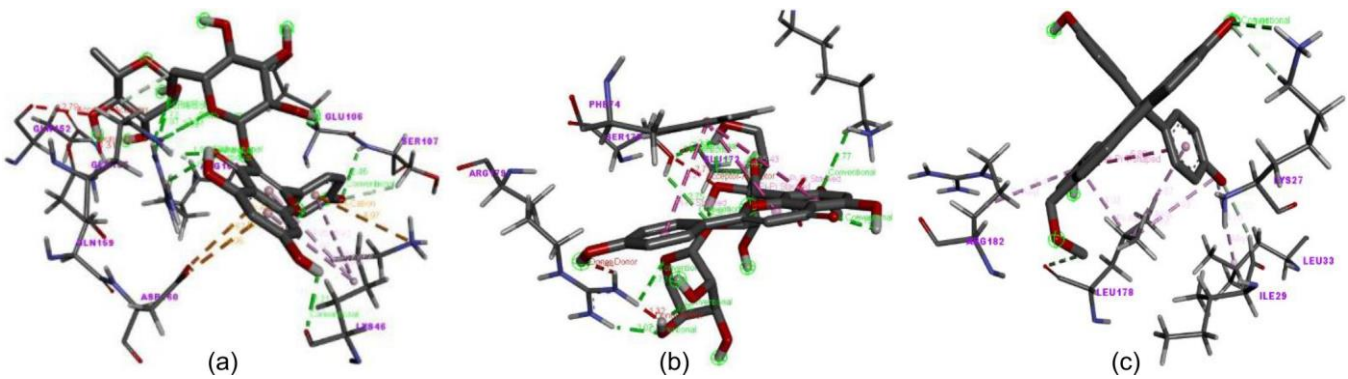

Fig. 5. 3D interaction images of (a) kaempferol-3-*o*-rutinoside, (b) 8-[4,5-dihydroxy-6-(hydroxymethyl)-3-[3,4,5-trihydroxy-6-(hydroxymethyl)oxan-2-yl]oxyoxan-2-yl]-5,7-dihydroxy-2-(4-hydroxyphenyl)chromen-4-one and (c) selaginpulvilin T with Human Interleukin-6 (PDB: 1ALU)

TABLE-4
INTERACTION OF PHYTOCOMPOUNDS WITH IL4 (PDB: 3BPN)

Code	BA	Interacting residues	Type of interactions	Distance
Lignoceric acid	-4.1	Asn130	Conventional hydrogen bond	2.42
		Gln8	Conventional hydrogen bond	2.48
		Phe259	Alkyl, π-Alkyl	5.11
		Lys318	Alkyl, π-Alkyl	4.43, 4.88
Phosphatidylcholine lyso alkyl 18	-5.4	Arg88	Salt Bridge	2.62
		Lys84	Attractive charge	5.22
		Arg88	Conventional hydrogen bond	2.62
		Lys84	Conventional hydrogen bond	2.34, 2.74
		Leu42	Conventional hydrogen bond	3.53
		Arg81	Alkyl, π-Alkyl	4.92
		Ile80	Alkyl, π-Alkyl	4.81
		Lys77	Alkyl, π-Alkyl	3.99, 4.41, 4.71
		Phe73	Alkyl, π-Alkyl	4.47, 5.04
		Leu66	Alkyl, π-Alkyl	4.53, 5.31
5-Hydroxytryptophan	-6.1	Gln8	Conventional hydrogen bond	2.30
		Lys12	Conventional hydrogen bond	1.94
		His131	Conventional hydrogen bond	3.76
		Leu319	π-Sigma	3.96
		Lys12	π-Alkyl	5.00
		Leu319	π-Alkyl	5.18
Quinic acid	-5.8	Val68	Conventional hydrogen bond	1.93
		Arg85	Conventional hydrogen bond	2.54
		Tyr13	Conventional hydrogen bond	1.94
		Asn126	Conventional hydrogen bond	2.20
		Asp125	Conventional hydrogen bond	3.37
D-(+)-Trehalose	-6.1	Glu283	Conventional hydrogen bond	1.95
		Tyr244	Conventional hydrogen bond	2.06
		Lys281	Conventional hydrogen bond	2.32, 2.41
Shikimate	-5.5	Gln8	Conventional hydrogen bond	1.89
		Asn15	Conventional hydrogen bond	2.33
Spectinomycin	-6.9	Asp324	Conventional hydrogen bond	2.13, 2.19
		Lys318	Conventional hydrogen bond	2.39, 2.73
		Phe259	Alkyl, π-Alkyl	5.09
		Leu319	Alkyl, π-Alkyl	5.00
		His131	Alkyl, π-Alkyl	5.21
Hydroquinidine	-6.4	Lys12	Conventional hydrogen bond	2.01
		Tyr129	Conventional hydrogen bond	3.61
		Leu319	Alkyl, π-Alkyl	4.70
		Lys318	Alkyl, π-Alkyl	5.41
		Leu155	Alkyl, π-Alkyl	4.88
		Pro124	Alkyl, π-Alkyl	5.40
		Lys12	Alkyl, π-Alkyl	3.90, 4.80
7,4'-Dimethoxyisoflavone	-7.2	His59	Conventional hydrogen bond	2.56
		Lys109	Conventional hydrogen bond	2.25
		Thr30	Conventional hydrogen bond	2.57
		Glu106	π-Anion	4.33
		Val29	π-Sigma	3.80
		Val51	Alkyl	4.45
Sorbate	-4.7	Lys318	Conventional hydrogen bond	2.64
		Leu319	Conventional hydrogen bond	2.43
		Leu319	Alkyl, π-Alkyl	4.19
		Lys12	Alkyl, π-Alkyl	3.81, 5.06
		His131	Alkyl, π-Alkyl	4.88
Harman	-6.6	His131	Conventional hydrogen bond	3.61
		Lys12	π-Cation	4.81
		Lys318	Alkyl, π-Alkyl	4.65
		Lys12	Alkyl, π-Alkyl	3.87
		His131	Alkyl, π-Alkyl	5.23
		Leu319	Alkyl, π-Alkyl	4.45, 4.91, 5.06

9-Hydroxy-10,12-octadecadienoic acid	-4.8	Lys318	Conventional hydrogen bond	2.17, 2.47
		Asp324	Conventional hydrogen bond	2.53
		Lys12	Alkyl	3.82
		Lys318	Alkyl	4.09
		Leu319	Alkyl	2.23
Kaempferol-3-*o*-rutinoside	-8.1	Gln106	Conventional hydrogen bond	2.11
		Glu103	Conventional hydrogen bond	2.35
		Thr30	Conventional hydrogen bond	2.63
		Thr28	Conventional hydrogen bond	2.14, 2.24, 2.74
		Gln54	Conventional hydrogen bond	3.64
		His58	Conventional hydrogen bond	3.33
		Glu106	π-Anion	3.93
		Leu27	π-Alkyl	4.79
2',4'-Dihydroxy-4-methoxychalcone	-6.8	Glu283	Conventional hydrogen bond	2.11
		Thr153	Conventional hydrogen bond	2.21
		Tyr244	π-π Stacked	3.85
Methyl-13-hydroperoxy-delta9E,11E-octadecadienoate	-4.4	Lys12	Alkyl	5.13, 5.40
		Leu319	Alkyl	4.28
		Lys318	Alkyl	4.05, 4.51
Cholestane	-8.6	Lys84	Alkyl	5.39
		Lys77	Alkyl	4.06, 4.84
		Leu39	Alkyl	4.43
		Ile80	Alkyl	5.17
Altenusin	-7.1	Asn15	Conventional hydrogen bond	2.07
		Gln8	Conventional hydrogen bond	2.89
		Lys12	Conventional hydrogen bond	3.52
		Lys318	π-Alkyl	4.15
		Lys12	π-Alkyl	5.06
		Leu319	π-Alkyl	5.05
8-[4,5-Dihydroxy-6-(hydroxymethyl)-3-[3,4,5-trihydroxy-6-(hydroxymethyl)oxan-2-yl]oxyoxan-2-yl]-5,7-dihydroxy-2-(4-hydroxyphenyl)chromen-4-one	-9.2	Pro124	Conventional hydrogen bond	2.63
		Lys12	Conventional hydrogen bond	2.59, 2.68
		Tyr127	Conventional hydrogen bond	2.40
		Leu319	Conventional hydrogen bond	2.57
		Asp324	Conventional hydrogen bond	2.45
		Lys318	Conventional hydrogen bond	1.96, 2.49
		His131	π-Cation	4.78
		Lys12	π-Sigma	3.49
		Lys318	π-Alkyl	4.72
		Leu319	π-Alkyl	5.11
Selaginpulvilin T	-7.6	Glu322	Conventional hydrogen bond	2.16
		Arg115	Conventional hydrogen bond	1.95
		Asp75	π-Anion	4.75
		Glu110	π-Anion	3.26, 4.53
		Glu114	π-Anion	3.33
		Pro221	π-Alkyl	5.36

Lys12, His131 and Leu319, through hydrogen bonds, C-H bonds and π-cation interactions. Moreover, spectinomycin (-6.9 kcal/mol) displayed multiple conventional hydrogen bonds with Asp324 and Lys318, along with alkyl and π-alkyl interactions with Phe259 and His131. On the lower binding affinity spectrum, lignoceric acid (-4.1 kcal/mol) and methyl-13-hydroperoxy-delta9E,11E-octadecadienoate (-4.4 kcal/mol) exhibited weak interactions, predominantly involving conventional hydrogen bonding and alkyl interactions with Lys318 and Leu319. Despite their lower affinity, these compounds might still contribute to stabilizing interactions within the binding pocket. Notably, phosphatidylcholine lyso alkyl 18 (-5.4 kcal/mol) formed a unique salt bridge with Arg88, indicating strong electrostatic interactions (Fig. 6).

IL-17 (PDB: 7UWL): Molecular docking analysis of various ligands with PDB: 7UWL also revealed a range of binding affinities and interaction profiles, highlighting key residues involved in binding (Table-5). Among the tested compounds, kaempferol-3-O-rutinoside (-7.8 kcal/mol) exhibited the strongest binding affinity, forming hydrogen bonds with ASP260 and interacting with GLU129 through a π-anion interaction. Other flavonoid derivatives, such as 8-[4,5-dihydroxy-6-(hydroxymethyl)-3-[3,4,5-trihydroxy-6-(hydroxymethyl)oxan-2-yl]oxyoxan-2-yl]-5,7-dihydroxy-2-(4-hydroxyphenyl)chrome-4-one (-7.5 kcal/mol) along with selaginpulvilin T (-7.2 kcal/mol), also represents strong affinities, engaging in hydrogen bonding and extensive π-π stacking interactions. Notably, hydroquinidine (-6.7 kcal/mol), spectino-

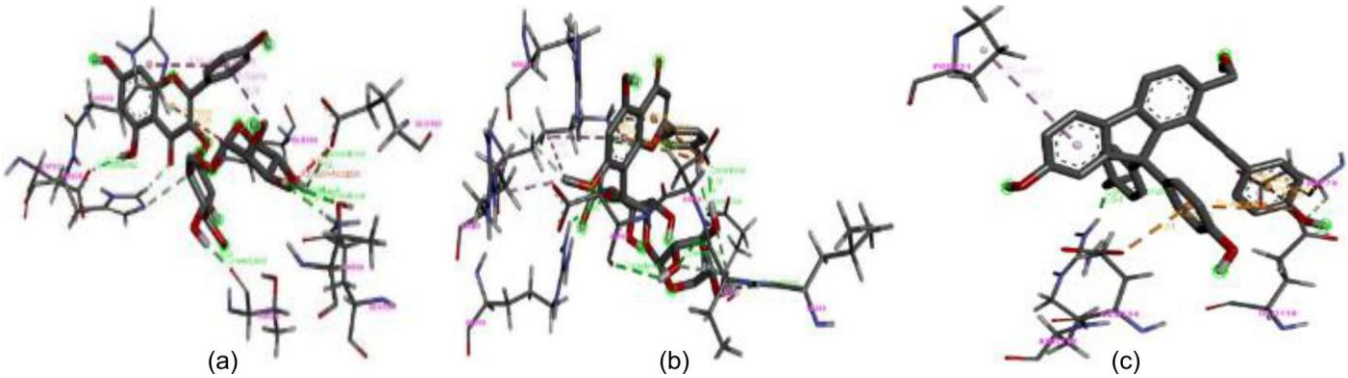

Fig. 6. 3D interaction images of (a) kaempferol-3-*o*-rutinoside, (b) 8-[4,5-dihydroxy-6-(hydroxymethyl)-3-[3,4,5-trihydroxy-6-(hydroxymethyl)oxan-2-yl]oxyoxan-2-yl]-5,7-dihydroxy-2-(4-hydroxyphenyl)chromen-4-one and (c) selaginpulvilin T with IL4 (PDB: 3BPN)

TABLE-5
INTERACTION OF PHYTOCOMPOUNDS WITH IL-17 (PDB: 7UWL)

Code	BA	Interacting residues	Type of interactions	Distance
Lignoceric acid	-3.7	HIS162	Conventional hydrogen bond	2.07
		SER115	Conventional hydrogen bond	2.92
		THR160	Conventional hydrogen bond	2.90
		HIS175	Pi-Sigma	3.61
		HIS162	Alkyl, Pi-Alkyl	5.35
		PRO167	Alkyl, Pi-Alkyl	4.78, 5.11
		LYS166	Alkyl, Pi-Alkyl	3.91
Phosphatidylcholine lyso alkyl 18	-4.5	ARG124	Attractive charge	3.32
		ARG124	Conventional hydrogen bond	2.20
		HIS162	Conventional hydrogen bond	3.55
		LEU58	Conventional hydrogen bond	3.80
		LYS166	Alkyl, Pi-Alkyl	5.18
		HIS175	Alkyl, Pi-Alkyl	4.84, 5.02
		PRO167	Alkyl, Pi-Alkyl	4.54, 5.28, 5.43
		PRO173	Alkyl, Pi-Alkyl	5.25, 5.36
5-Hydroxytryptophan	-5.9	SER96	Conventional hydrogen bond	2.38, 2.45
		SER92	Conventional hydrogen bond	1.96
		TYR134	Conventional hydrogen bond	2.50
		PHE94	Pi-Pi Stacked	3.94, 3.99
Quinic acid	-5.5	GLN216	Conventional hydrogen bond	2.31
		HIS215	Conventional hydrogen bond	2.04, 2.19
		ARG271	Conventional hydrogen bond	2.03
		LEU273	Conventional hydrogen bond	1.94
		HIS279	Conventional hydrogen bond	2.63
D-(+)-Trehalose	-5.9	ASP293	Conventional hydrogen bond	2.72
		PRO153	Conventional hydrogen bond	2.50
		SER199	Conventional hydrogen bond	2.31, 2.49
		PRO195	Conventional hydrogen bond	2.69
		SER198	Conventional hydrogen bond	2.60, 2.74
		CYS196	Conventional hydrogen bond	2.79
Shikimate	-5.4	ASP149	Conventional hydrogen bond	1.87
		LYS74	Conventional hydrogen bond	2.37
		GLN101	Conventional hydrogen bond	2.66, 2.79
		ARG73	Conventional hydrogen bond	2.04
		ASP103	Conventional hydrogen bond	1.82, 2.07
Spectinomycin	-6.5	CYS196	Conventional hydrogen bond	2.63
		SER199	Conventional hydrogen bond	1.91, 2.58
		GLN155	Conventional hydrogen bond	2.60
		ASP293	CH bond	3.68

Hydroquinidine	-6.7	PRO127	Conventional hydrogen bond	2.44
		SER96	CH bond	3.77
		GLU129	Pi-Anion	3.65
		VAL88	Alkyl, Pi-Alkyl	4.89
		PHE126	Alkyl, Pi-Alkyl	5.30
		PRO127	Alkyl, Pi-Alkyl	4.39
7,4'-Dimethoxyisoflavone	-6.9	SER92	CH bond	3.49
		PHE94	Pi-Pi Stacked	4.10, 4.51
		TYR134	Pi-Alkyl	5.38
Sorbate	-4.5	SER96	Conventional hydrogen bond	2.00
		SER98	Conventional hydrogen bond	2.67
		VAL100	Alkyl, Pi-Alkyl	4.73
		PHE126	Alkyl, Pi-Alkyl	3.86, 4.21
Harman	-6.5	GLU129	Pi-Anion	2.28
		GLU129	Pi-Sigma	2.91
		PHE94	Pi-Pi Stacked	3.31
		TYR134	Pi-Alkyl	1.96
9-Hydroxy-10,12-octadecadienoic acid	-4.7	PHE94	Alkyl, Pi-Alkyl	4.68, 5.22
		LEU161	Alkyl, Pi-Alkyl	4.22
Kaempferol-3-*o*-rutinoside	-7.8	ASP260	Conventional hydrogen bond	2.55
		CYS257	CH bond	2.29
		GLU129	Pi-Anion	4.82
		LYS172	Pi-Alkyl	5.18
2',4'-Dihydroxy-4-methoxychalcone	-6.-1	TYR134	Conventional hydrogen bond	2.16
		PRO127	CH bond	2.90
		PHE94	Pi-Pi Stacked	4.59, 4.89
		PRO127	Pi-Alkyl	4.69
Methyl-13-hydroperoxy-delta9E,11E-octadecadienoate	-5.3	LYS172	Conventional hydrogen bond	2.27
		SER92	Conventional hydrogen bond	2.06
		THR132	CH bond	2.53
		TYR134	CH bond	3.56
		LYS91	CH bond	2.89
		ILE64	Alkyl, Pi-Alkyl	4.56
		PHE94	Alkyl, Pi-Alkyl	4.62
		LYS170	Alkyl, Pi-Alkyl	4.39
		LEU130	Alkyl, Pi-Alkyl	4.23, 4.31
		LYS172	Alkyl, Pi-Alkyl	4.79, 5.11
Cholestane	-7.3	PHE94	Pi-Sigma	3.81
		TYR134	Pi-Alkyl	4.99
		PHE94	Pi-Alkyl	4.68
Altenusin	-6.3	CYS196	Conventional hydrogen bond	2.73
		SER198	Conventional hydrogen bond	1.85
		CYS290	Pi-Sulfur	4.00, 5.99
		LEU295	Alkyl, Pi-Alkyl	4.93, 5.35
		CYS185	Alkyl, Pi-Alkyl	5.30
8-[4,5-Dihydroxy-6-(hydroxymethyl)-3-[3,4,5-trihydroxy-6-(hydroxymethyl)oxan-2-yl]oxyoxan-2-yl]-5,7-dihydroxy-2-(4-hydroxyphenyl)chromen-4-one	-7.5	SER92	Conventional hydrogen bond	2.48
		TYR134	Conventional hydrogen bond	2.34
		SER96	CH bond	2.43, 2.73
		PHE94	Pi-Pi Stacked	3.90, 4.62
Selaginpulvilin T	-7.2	TRP62	Conventional hydrogen bond	2.13
		GLY171	Conventional hydrogen bond	2.15
		ARG124	Conventional hydrogen bond	2.28
		HIS162	CH bond	2.91
		HIS163	CH bond	3.31
		ASP59	CH bond	3.47
		PRO167	Pi-Pi T-Shaped	4.98
		HIS175	Amide-Pi Stacked	4.84
		LYS166	Alkyl, Pi-Alkyl	3.78, 5.04
		HIS162	Alkyl, Pi-Alkyl	5.36
		PRO167	Alkyl, Pi-Alkyl	4.45, 4.82

mycin (-6.5 kcal/mol), along harman (-6.5 kcal/mol) demonstrated moderate binding, involving π-anion, hydrogen bonds, along with alkyl interactions with residues like GLU129, PHE94 and TYR134. Conversely, fatty acids such as lignoceric acid (-3.7 kcal/mol) and 9-hydroxy-10,12-octadecadienoic acid (-4.7 kcal/mol) exhibited lower affinities, primarily interacting through alkyl and π-alkyl interactions with residues including HIS162, PRO167 and LYS166. Interestingly, D-(+)-trehalose (-5.9 kcal/mol) and shikimate (-5.4 kcal/mol) developed multiple conventional hydrogen bonds, particularly accompanied by ASP293 and GLN101, suggesting possible hydrogen bonding-driven stability (Fig. 7). These findings indicate that polyphenolic and flavonoid compounds, particularly kaempferol-3-O-rutinoside, exhibit strong interactions with 7UWL, potentially influencing its biological function through stabilizing interactions with key residues.

IL-13 (PDB: 5KNH): Docking studies with PDB: 5KNH revealed major variations in binding affinities and interaction profiles among the tested compounds. Results provided insights into their potential binding modes and stability within the target site (Table-6). The highest binding affinity was observed for kaempferol-3-O-rutinoside (-6.9 kcal/mol) and cholestane (-6.9 kcal/mol), forming multiple stabilizing interactions. Kaempferol-3-O-rutinoside exhibited conventional hydrogen bonds with GLN94 and ALA26, CH bonds with GLN94 and ALA93 and π-alkyl interactions with ALA26, LYS97 and ALA93, contributing to its strong affinity. Similarly, cholestane interacted primarily through hydrophobic forces, engaging in alkyl and π-alkyl interactions with LEU39, VAL101, PHE145, LYS147 and ILE152, highlighting its potential as a lipophilic binder. Among flavonoid derivatives, 8-[4,5-dihydroxy-6-(hydroxymethyl)-3-[3,4,5-trihydroxy-6-(hydroxy-

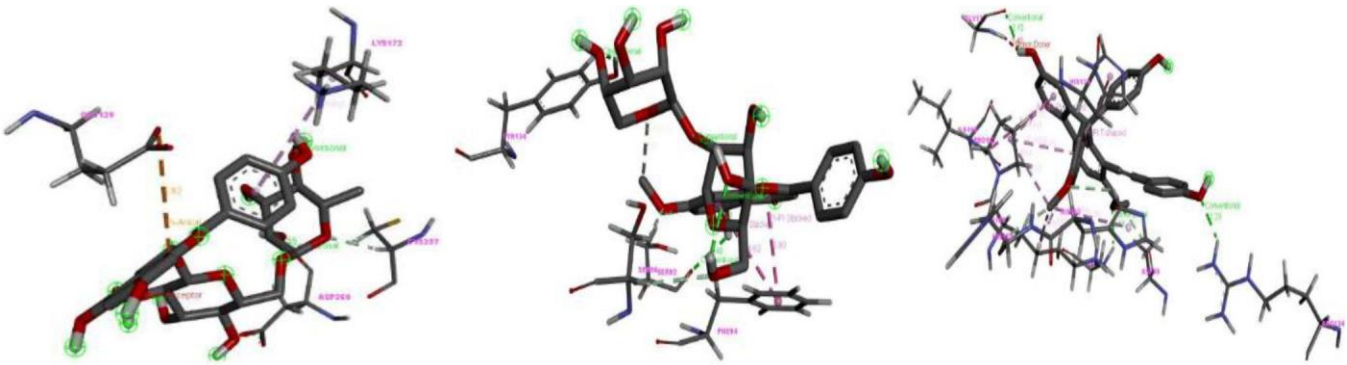

Fig. 7. 3D interaction images of (a) kaempferol-3-*o*-rutinoside, (b) 8-[4,5-dihydroxy-6-(hydroxymethyl)-3-[3,4,5-trihydroxy-6-(hydroxymethyl)oxan-2-yl]oxyoxan-2-yl]-5,7-dihydroxy-2-(4-hydroxyphenyl)chromen-4-one and (c) selaginpulvilin T with IL-17 (PDB: 7UWL)

TABLE-6
INTERACTION OF PHYTOCOMPOUNDS WITH IL-13 (PDB: 5KNH)

Code	BA	Interacting residues	Type of interactions	Distance
Lignoceric acid	-3.7	SER7	Conventional hydrogen bond	2.71
		TYR46	Conventional hydrogen bond	2.07
		SER45	Conventional hydrogen bond	2.01
		LEU19	Alkyl	4.18
Phosphatidylcholine lyso alkyl 18	-5	GLU20	Attractive charge	5.34
		ASP44	Attractive charge	4.71
		ASN113	Attractive charge	4.97
		TYR46	Conventional hydrogen bond	2.48
		PHE112	Conventional hydrogen bond	3.55
		ASP44	Conventional hydrogen bond	3.40
		LEU106	Alkyl, Pi-Alkyl	4.46
		VAL143	Alkyl, Pi-Alkyl	5.19, 5.22, 5.42
		PRO6	Alkyl, Pi-Alkyl	4.74
		PHE112	Alkyl, Pi-Alkyl	4.47, 4.52
5-Hydroxytryptophan	-6.2	GLN22	Conventional hydrogen bond	2.54
		GLN24	Conventional hydrogen bond	2.20
		THR21	Pi-Sigma	2.53
		LEU28	Pi-Alkyl	5.47
		ALA93	Pi-Alkyl	3.80, 4.72
		ALA26	Pi-Alkyl	4.97, 3.94
Quinic acid	-5.3	GLN122	Conventional hydrogen bond	2.84
		LYS97	Conventional hydrogen bond	2.74

D-(+)-trehalose	-5.8	THR21	Conventional hydrogen bond	1.97
		ALA93	Conventional hydrogen bond	2.79
		LYS144	Conventional hydrogen bond	2.70
		THR21	Conventional hydrogen bond	2.48, 3.35
Shikimate	-5	GLN122	Conventional hydrogen bond	2.51
		LYS97	Conventional hydrogen bond	2.04
		ASP155	Conventional hydrogen bond	2.30
Spectinomycin	-6.2	GLN22	Conventional hydrogen bond	2.43
		GLN94	Conventional hydrogen bond	3.08
		GLN24	Conventional hydrogen bond	3.44
Hydroquinidine	-6.3	GLN94	Conventional hydrogen bond	2.82
		GLN94	Conventional hydrogen bond	2.30
		LYS97	Alkyl, Pi-Alkyl	4.81
		ILE20	Alkyl, Pi-Alkyl	5.40
		LEU28	Alkyl, Pi-Alkyl	4.10
		ALA93	Alkyl, Pi-Alkyl	3.76, 5.33
		PRO27	Alkyl, Pi-Alkyl	3.74
		ALA26	Alkyl, Pi-Alkyl	3.80, 4.97
		PHE145	Alkyl, Pi-Alkyl	5.27
7,4'-Dimethoxyisoflavone	-6.6	LYS97	Conventional hydrogen bond	2.00
		LYS147	Conventional hydrogen bond	1.90
		ASN156	Conventional hydrogen bond	3.61
		VAL101	Alkyl, Pi-Alkyl	3.83, 4.56, 5.40
		ILE152	Alkyl, Pi-Alkyl	5.09, 5.16
Sorbate	-5.3	LYS104	Salt Bridge	4.47
		ARG108	Attractive charge	2.03
		GLN122	Conventional hydrogen bond	2.04
		ARG108	Conventional hydrogen bond	2.19
		LYS147	Alkyl, Pi-Alkyl	4.42
		ILE152	Alkyl, Pi-Alkyl	5.12
		VAL101	Alkyl, Pi-Alkyl	4.38
		PHE145	Alkyl, Pi-Alkyl	4.65, 5.26
Harman	-6.2	THR21	Pi-Sigma	2.60
		PHE145	Pi-Pi Stacked	5.70
		LEU28	Pi-Alkyl	5.08
		ALA26	Pi-Alkyl	4.61, 4.96
		ALA93	Pi-Alkyl	3.57, 4.21
		LYS97	Pi-Alkyl	5.13
9-Hydroxy-10,12-octadecadienoic acid	-5.2	ASN156	Conventional hydrogen bond	2.60, 2.61
		GLN122	Conventional hydrogen bond	2.35
		LEU39	Alkyl, Pi-Alkyl	4.32
		HIS102	Alkyl, Pi-Alkyl	4.27, 5.45
		VAL101	Alkyl, Pi-Alkyl	4.42, 4.65, 5.45
		ILE152	Alkyl, Pi-Alkyl	5.04
Kaempferol-3-*o*-rutinoside	-6.9	GLN94	Conventional hydrogen bond	2.44
		ALA26	Conventional hydrogen bond	3.02
		GLN94	Conventional hydrogen bond	2.54
		ALA93	Conventional hydrogen bond	2.59
		ALA26	Pi-Alkyl	5.45
		LYS97	Pi-Alkyl	5.49
		ALA93	Pi-Alkyl	4.16
2',4'-Dihydroxy-4-methoxychalcone	-6.1	LYS97	Conventional hydrogen bond	2.96
		LEU28	Pi-Alkyl	5.48
		ALA26	Pi-Alkyl	4.74
		ALA93	Pi-Alkyl	3.71, 5.07
Methyl-13-hydroperoxy-delta9E,11E-octadecadienoate	-4.9	GLN94	Conventional hydrogen bond	1.91
		LYS97	Conventional hydrogen bond	2.02, 2.72
		ASP155	Conventional hydrogen bond	3.58
		LYS104	Alkyl	3.95
		VAL101	Alkyl	3.60, 4.22, 4.69, 5.02

Cholestane	-6.9	LEU39	Alkyl, Pi-Alkyl	5.10, 5.41
		VAL101	Alkyl, Pi-Alkyl	4.14, 4.68
		PHE145	Alkyl, Pi-Alkyl	4.64
		LYS147	Alkyl, Pi-Alkyl	4.92
		ILE152	Alkyl, Pi-Alkyl	5.15
Altenusin	-6.1	LYS97	Pi-Cation	3.83
		LYS105	Pi-Cation	3.89
		VAL101	Alkyl, Pi-Alkyl	3.97, 4.66, 4.84
		ILE152	Alkyl, Pi-Alkyl	5.20
8-[4,5-Dihydroxy-6-(hydroxymethyl)-3-[3,4,5-trihydroxy-6-(hydroxymethyl)oxan-2-yl]oxyoxan-2-yl]-5,7-dihydroxy-2-(4-hydroxyphenyl)chromen-4-one	-6.7	ILE20	Conventional hydrogen bond	2.34
		THR21	Conventional hydrogen bond	2.67
		GLN22	Conventional hydrogen bond	2.22, 2.44, 2.63
		GLN24	Conventional hydrogen bond	2.70
		LYS97	Conventional hydrogen bond	2.55
		PHE145	Conventional hydrogen bond	3.79
		ALA26	Pi-Alkyl	4.61
		ALA93	Pi-Alkyl	3.75
Selaginpulvilin T	-6.7	PRO6	Conventional hydrogen bond	2.59
		VAL4	Conventional hydrogen bond	3.39
		GLN111	Conventional hydrogen bond	3.70
		CYS45	Pi-Sulfur	4.95
		PHE70	Alkyl, Pi-Alkyl	5.08
		ALA9	Alkyl, Pi-Alkyl	3.64, 5.33
		PRO6	Alkyl, Pi-Alkyl	4.23, 5.14

methyl)-oxan-2-yl]oxyoxan-2-yl]-5,7-dihydroxy-2-(4-hydroxyphenyl)chromen-4-one (-6.7 kcal/mol) and selaginpulvilin T (-6.7 kcal/mol) exhibited strong interactions, forming hydrogen bonds with GLN22, GLN24, LYS97 and THR21, along with CH and π-alkyl interactions that contributed to their stability. 7,4′-dimethoxyisoflavone (-6.6 kcal/mol) also demonstrated strong binding, engaging LYS97, LYS147 and ASN156 in hydrogen and CH bonds, with additional hydrophobic interactions with VAL101 and ILE152. Hydroquinidine (-6.3 kcal/mol), harman (-6.2 kcal/mol), spectinomycin (-6.2 kcal/mol) and 5-hydroxytryptophan (-6.2 kcal/mol) exhibited moderate affinities, forming conventional hydrogen bonds with key residues such as GLN94, GLN22, GLN24 and THR21. These compounds also displayed π-alkyl and alkyl interactions, particularly with ALA93, ALA26 and LEU28, indicating stable binding through a mixture of hydrophilic and hydrophobic interactions. Among other notable compounds, D-(+)-trehalose (-5.8 kcal/mol), shikimate (-5.0 kcal/mol) and quinic acid (-5.3 kcal/mol) established multiple hydrogen bonds with GLN122, LYS97, ASP155 and THR21, suggesting a hydrogen bonding-driven binding mechanism. Phosphatidylcholine lyso-alkyl 18 (-5.0 kcal/mol) primarily interacted through attractive charge interactions with GLU20, ASP44 and ASN113, along with π-alkyl interactions with LEU106, VAL143 and PHE112. Interestingly, fatty acids such as lignoceric acid (-3.7 kcal/mol) and 9-hydroxy-10,12-octadecadienoic acid (-5.2 kcal/mol) exhibited weaker affinities, primarily engaging in conventional hydrogen bonding with SER7, TYR46 and ASN156, alongside alkyl interactions with HIS102, LEU19 and VAL101 (Fig. 8). The relatively lower affinity suggests a lack of strong stabilizing interactions compared to polyphenolic compounds. These findings emphasize the significance of flavonoids and polyphenolic compounds as potential lead molecules due to their superior binding affinities and interaction networks, particularly through hydrogen bonding and hydrophobic interactions. Future studies should focus on validating these computational predictions through *in vitro* and analyze *in vivo* to assess their biological relevance and therapeutic potential.

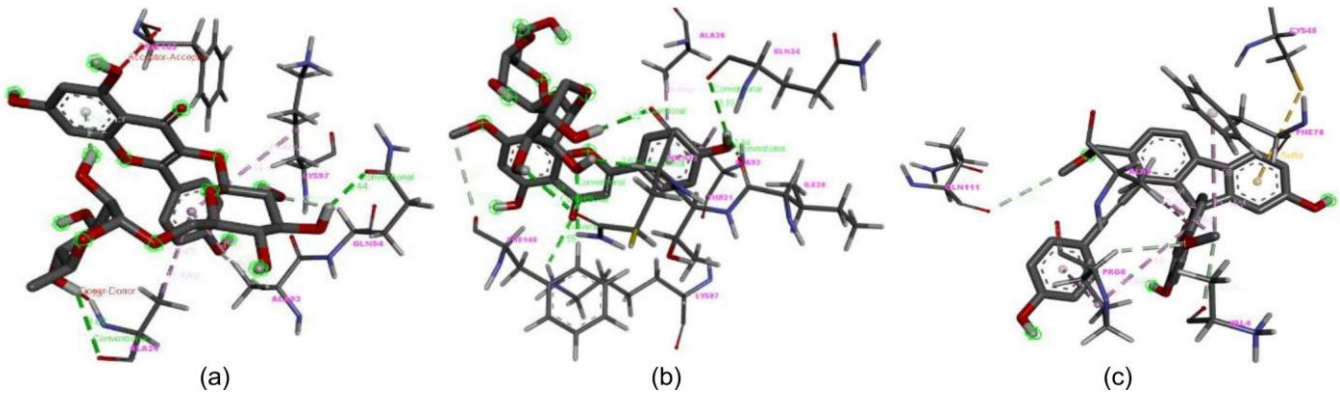

Fig. 8. 3D interaction images of (a) kaempferol-3-*o*-rutinoside, (b) 8-[4,5-dihydroxy-6-(hydroxymethyl)-3-[3,4,5-trihydroxy-6-(hydroxymethyl)oxan-2-yl]oxyoxan-2-yl]-5,7-dihydroxy-2-(4-hydroxyphenyl)chromen-4-one and (c) selaginpulvilin T with IL-13 (PDB: 5KNH)

TABLE-7
ADMET STUDY OF PHYTOCOMPOUNDS

Property	Predicted values											
	A	**B**	**C**	**D**	**E**	**F**	**G**	**H**	**I**	**J**	**K**	**L**
Molecular weight	342.3	332.35	326.43	111.12	174.15	192.17	220.22	290.27	182.22	270.28	282.29	296.44
Number of rotatable bonds	4	2	4	2	1	1	3	3	0	4	3	14
Number of hydrogen acceptors	11	9	4	2	5	6	4	6	1	4	4	3
Number of hydrogen donors	8	5	1	0	4	5	4	4	1	2	0	2
Molar refractivity	68.12	75.65	100.21	29.84	38.43	40.11	59.38	76.36	58.57	76.79	80.9	90.63
TPSA	189.53	129.51	45.59	40.13	97.99	118.22	99.34	107.22	28.68	66.76	48.67	57.53
mLogP	-4.37	-2.44	2.31	1.07	-1.43	-2.14	-2.22	1.37	1.9	1.83	1.57	3.59
LogS	0.81	0.93	-3.73	-1.77	0.18	0.43	-0.42	-4.81	-3.56	-4.8	-4.64	-6.31
Lipinski's rule	2	0	0	0	0	0	0	0	0	0	0	0
Ghose rule	1	1	0	3	2	1	0	0	0	0	0	0
Veber rule	1	0	0	0	0	0	0	0	0	0	0	1
Egan rule	1	0	0	0	0	0	0	0	0	0	0	0
Muegge rule	4	1	0	1	1	2	0	0	1	0	0	1
Bioavailability score	0.17	0.55	0.55	0.85	0.56	0.56	0.56	0.55	0.55	0.55	0.55	0.85
Ames toxicity	No	No	No	No	No	No	No	No	Yes	Yes	Yes	No
Hepatotoxicity	No	No	Yes	No	No	No	No	No	No	No	No	No

A = 7427: Trehalose; **B** = 15541: Spectinomycin; **C** = 91503: Hydroquinidine; **D** = 1549237: Sorbate; **E** = 8742: Shikimate; **F** = 6508: Quinic acid; **G** = 144: 5-Hydroxytryptophan; **H** = 6918469: Altenusin; **I** = 5281404: Harman; **J** = 5711223: 2',4'-Dihydroxy-4-Methoxychalcone; **K** = 466269: 7,4'-Dimethoxyisoflavone; **L** = 5282945: 9-Hydroxy-10,12-octadecadienoic acid

ADMET study: The ADMET properties of the twelve phytocompounds were evaluated to assess their pharmacokinetic potential, as suboptimal ADMET profiles can limit the clinical development and approval of therapeutic agents. The ADMET profile of 12 different compounds is represented in Table-7 as an *in silico* assessment of the ADMET of remaining molecules was not possible due to its higher molecular weight.

Conclusion

The *in vitro* study of hydroalcoholic extract of *Tabernaemontana* divaricata (TDHE) reveals its therapeutic potential against asthma. HR-LC MS/MS analysis revealed a significant presence of terpenoid, phenolic and alkaloidal compounds in the chemical profile of extract. The molecular docking study reveals the potential activity of secondary metabolites such as kaempferol-3-*o*-rutinoside,8-[4,5-dihydroxy-6-(hydroxymethyl)-3-[3,4,5-trihydroxy-6-(hydroxymethyl)oxan-2-yl]oxyoxan-2-yl]-5,7-dihydroxy-2-(4-hydroxyphenyl)chromen-4-one and phenol selaginpulvilin T against targeted proteins of asthma likewise H1, IL-6, IL-4, IL-17 and IL-13. A molecular docking study indicated that the compounds may possess enhanced antiasthmatic potential with a multitargeted approach, as demonstrated by their robust interactions with pertinent proteins.

ACKNOWLEDGEMENTS

The authors thank Dr. Manoj Charde for support during research work.

CONFLICT OF INTEREST

The authors declare that there is no conflict of interests regarding the publication of this article.

DECLARATION OF AI-ASSISTED TECHNOLOGIES

During the preparation of this manuscript, the authors used an AI-assisted tool(s) to improve the language. The authors reviewed and edited the content and take full responsibility for the published work.

REFERENCES

1. A. Haikal, M. El-Neketi, M.G. Helal, L.A. Abou-zeid, M.A. Hassan and A.A. Gohar, *J. Ethnopharmacol.*, **339**, 119133 (2025); https://doi.org/10.1016/j.jep.2024.119133
2. M.S. Ali Khan, Misbah, N. Ahmed, M. Arifuddin, A. Rehman and M.P. Ling, *Food Chem. Toxicol.*, **118**, 953 (2018); https://doi.org/10.1016/j.fct.2018.06.007
3. W. Pratchayasakul, A. Pongchaidecha, N. Chattipakorn and S. Chattipakorn, *Indian J. Med. Res.*, **127**, 317 (2008).
4. M.S.A. Khan, Misbah, N. Ahmed, M. Arifuddin, A. Rehman and M. P. Ling, *Food Chem. Toxicol.*, **118**, 953 (2018); https://doi.org/10.1016/j.fct.2018.06.007
5. A.K. Srivastava, H. Nagar, R. Srivastava, V. Ahirwar and H.S. Chandel, *Ayu*, **37**, 256 (2016); https://doi.org/10.4103/ayu.AYU_35_16
6. Z. Yabré, R. Boly, R. Ouédraogo, A.G.V. Coulidiaty, G.D. Somda, R. Semdé, N. Ouédraogo and E.N.H. You, *Heliyon*, **10**, e32402 (2024); https://doi.org/10.1016/j.heliyon.2024.e32402.
7. R.G. Mali and A.S. Dhake, *Orient. Pharm. Exp. Med.*, **11**, 77 (2011); https://doi.org/10.1007/s13596-011-0019-1
8. A. Boboltz, S. Kumar and G.A. Duncan, *Adv. Drug Deliv. Rev.*, **198**, 114858 (2023); https://doi.org/10.1016/j.addr.2023.114858
9. N.A. Hanania and R.H. Moore, *Curr. Drug Targets Inflamm. Allergy*, **3**, 271 (2004); https://doi.org/10.2174/1568010043343598
10. P. Bradding, C. Porsbjerg, A. Côté, S.-E. Dahlén, T.S. Hallstrand and C.E. Brightling, *J. Allergy Clin. Immunol.*, **153**, 1181 (2024); https://doi.org/10.1016/j.jaci.2024.02.011
11. A. Memarzia, F. Amin, S. Saadat, M. Jalali, Z. Ghasemi and M.H. Boskabady, *J. Ethnopharmacol.*, **241**, 1120 (2019); https://doi.org/10.1016/j.jep.2019.112012
12. A. Haikal, M. El-Neketi, M.G. Helal, L.A. Abou-zeid, M.A. Hassan and A.A. Gohar, *J. Ethnopharmacol.*, **13**, 339 (2025); https://doi.org/10.1016/j.jep.2024.119133

13. K.L. Ho, P.H. Yong, C.W. Wang, S.H. Lim, U.R. Kuppusamy, B. Arumugam, C.T. Ngo and Z.X. Ng, *Bioorg. Chem.*, **153**, 107969 (2024); https://doi.org/10.1016/j.bioorg.2024.107969
14. D. Zephy and J. Ahmad, *Diabetes Metab. Syndr.*, **9**, 127 (2015); https://doi.org/10.1016/j.dsx.2014.09.018
15. A.C. Maritim, R.A. Sanders and J.B. Watkins III, *J. Biochem. Mol. Toxicol.*, **17**, 24 (2003); https://doi.org/10.1002/jbt.10058
16. M.M. Hasan, M.E. Islam, M.S. Hossain, M. Akter, M.A.A. Rahman, M. Kazi, S. Khan and M.S. Parvin, *Heliyon*, **10**, e22972 (2024); https://doi.org/10.1016/j.heliyon.2023.e22972
17. 22 D.J. Taur, R.N. Patil and R.Y. Patil, *J. Tradit. Complement. Med.*, **7**, 428 (2017); https://doi.org/10.1016/j.jtcme.2016.12.007
18. R. Alam, J.A. Mazumder, S. Das and P.K.D. Mohapatra, *Bioresour. Technol. Rep.*, **29**, 102020 (2025); https://doi.org/10.1016/j.biteb.2025.102020
19. V. Unsal, E. Oner, R. Yıldız and B.D. Mert, *BMC Chem.*, **19**, 4 (2025); https://doi.org/10.1186/s13065-024-01371-4
20. H.A. Salman, A.S. Yaakop, S. Aladaileh, M. Mustafa, M. Gharaibeh and U.M. Kahar, *Heliyon*, **9**, e12730 (2023); https://doi.org/10.1016/j.heliyon.2022.e12730
21. S. Sarithamol, V. Divya, S. Surendran, V.L. Pushpa and K.B. Manoj, *Int. J. Curr. Pharm. Res.*, **10**, 43 (2018); https://doi.org/10.22159/ijcpr.2018v10i1.24704
22. S.C. Wilson, N.A. Caveney, M. Yen, C. Pollmann, X. Xiang, K.M. Jude, M. Hafer, N. Tsutsumi, J. Piehler and K.C. Garcia, *Nature*, **609**, 622 (2022); https://doi.org/10.1038/s41586-022-05116-y
23. P. Ntontsi, E. Papathanassiou, S. Loukides, P. Bakakos and G. Hillas, *Expert Opin. Investig. Drugs*, **27**, 179 (2018); https://doi.org/10.1080/13543784.2018.1427729
24. P. Kharade, D. Gaikwad, S. Rathod, U. Chougale, S. Kadam, K. Patil, P. Choudhari and S. Desai, *J. Mol. Liq.*, **416**, 126484 (2024); https://doi.org/10.1016/j.molliq.2024.126484
25. A. Daina, O. Michielin and V. Zoete, *Sci. Rep.*, **7**, 42717 (2017); https://doi.org/10.1038/srep42717
26. D.E.V. Pires, T.L. Blundell and D.B. Ascher, *J. Med. Chem.*, **58**, 4066 (2015); https://doi.org/10.1021/acs.jmedchem.5b00104
27. N.M. Peixoto Araujo, H.S. Arruda, F.N. dos Santos, D.R. de Morais, G.A. Pereira and G.M. Pastore, *Food Res. Int.*, **137**, 109 (2020); https://doi.org/10.1016/j.foodres.2020.109556